DOI: 10.1021/jm901614b

Journal of Medicinal Chemistry Article

Design, Synthesis, Biological Properties, and Molecular Modeling Investigations of Novel Tacrine Derivatives with a Combination of Acetylcholinesterase Inhibition and Cannabinoid CB_1 Receptor Antagonism

Jos H. M. Lange,* Hein K. A. C. Coolen, Martina A. W. van der Neut, Alice J. M. Borst, Bob Stork, Peter C. Verveer, and Chris G. Kruse

Solvay Pharmaceuticals, Research Laboratories, C. J. van Houtenlaan 36, 1381 CP Weesp, The Netherlands

Received November 3, 2009

Pyrazolines **7**−**10** were designed as novel CB_1 receptor antagonists, which exhibited improved turbidimetric aqueous solubilities. On the basis of their extended CB_1 antagonist pharmacophore, hybrid molecules exhibiting cannabinoid CB_1 receptor antagonistic as well as acetylcholinesterase (AChE) inhibiting activities were designed. The target compounds **12**, **13**, **20**, and **21** are based on **1** (tacrine) as the AChE inhibitor (AChEI) pharmacophore and two different CB_1 antagonistic pharmacophores. The imidazole-based **20** showed high CB_1 receptor affinity (48 nM) in combination with high CB_1/CB_2 receptor subtype selectivity (> 20-fold) and elicited equipotent AChE inhibitory activity as **1**. Molecular modeling studies revealed the presence of a binding pocket in the AChE enzyme which nicely accommodates the CB_1 pharmacophores of the target compounds **12**, **13**, **20**, and **21**.

Introduction

Alzheimer's disease (AD[a]) is a neurodegenerative disorder whose prevalence is increasing together with the life expectancy throughout the world. Cholinergic-enhancing drugs are the main current therapy.[1] The AChEI **1** was the first synthetic drug approved by the U.S. Food and Drug Administration for the treatment of AD (Figure 1). The tricyclic **1** is a reversible inhibitor that reduced the inactivation of acetylcholine (ACh).[2]

AChEIs[3] have shown efficacy not only in AD[4] but also in other cognitive disorders such as dementia with Lewy bodies,[5] Parkinson's disease,[6] vascular dementia,[7] traumatic brain injury,[8] and cognitive impairment in multiple sclerosis.[9]

Cognitive disorders constitute also a potential therapeutic area for cannabinoid CB_1 receptor antagonists,[10] since CB_1 receptor antagonists were shown to increase ACh release in certain brain areas including the cortical region and hippocampus.[11] On the basis of the observations that CB_1 receptor antagonists as well as AChEIs improved performance in a variety of animal memory models, Wise et al. found[12] that combined administration of subthreshold doses of the CB_1 receptor antagonist rimonabant and the AChEI donezepil, which had no discernible effects on performance when given alone, enhanced memory.

It was also found[13] that AChEIs acting on the brain suppressed both cocaine- and morphine-induced conditioned place preference and blocked the induction and persistence of cocaine-evoked hyperlocomotion. AChEIs can thus be approached as novel and potential therapeutic agents for drug addiction. Cannabinoid CB_1 receptor antagonists have also been associated[14] with the treatment of drug addiction and addictive behavior.

The multifactorial and complex ethiology of AD has hitherto prompted several so-called "single entity−multitarget ligand" approaches,[15] such as combined AChEI-histamine H_3 receptor antagonists,[16] dual binding site AChEIs,[17] NO-donor-AChEI hybrids,[18] tacrine−dihydropyridine hybrids,[19] tacrine−melatonin hybrids,[20] dual inhibitors of monoamine oxidase and AChE,[21] dual AChE/serotonin transporter inhibitors,[22] tacrine−ferulic acid hybrids,[23] and benzofuran-based hybrid compounds.[24]

Design

Molecular design which was based on our previous work on pyrazoline-based CB_1 receptor antagonists[25,26] such as **2** revealed that substitution of its amidine *N*-methyl group by sterically more demanding substituents would lead to compounds with retained CB_1 receptor antagonistic properties. First, this basic hypothesis is validated by the design of the target compounds **5**−**10** which contain either a polar group or an ionizable nitrogen atom in their amidine N substituent in order to produce novel CB_1 receptor antagonists with improved aqueous solubilities.

Second, the impact of both AChE inhibition and CB_1 receptor antagonism on cognitive deficits and drug addiction prompted the design of dual acting AChEIs/CB_1 receptor antagonists. Although the general concept of designing dual acting compounds based on **1** is not new as has been outlined above, our approach to dual acting compounds by combining the CB_1 antagonist pharmacophore with **1** is unprecedented and is of great importance because of the reported beneficial

*To whom correspondence should be addressed. Telephone: +31 (0)294 479731. Fax: +31 (0)294 477138. E-mail: jos.lange@solvay.com.

[a] Abbrevations: ACh, acetylcholine; AChE, acetylcholinesterase; AChEI, acetylcholinesterase inhibitor; AD, Alzheimer's disease; CHO, Chinese hamster ovary; DMAP, 4-dimethylaminopyridine; EDC, 1-(3-methylaminopropyl)-3-ethylcarbodiimide; GPCR, G-protein-coupled receptor; HEK, human embryonic kidney; HOAt, 1-hydroxy-7-azabenzotriazole; HRMS, high resolution mass spectrometry; NO, nitric oxide; PAS, peripheral anionic site; PDB, Protein Data Bank; SEM, standard error of the mean.

 Published on Web 01/04/2010

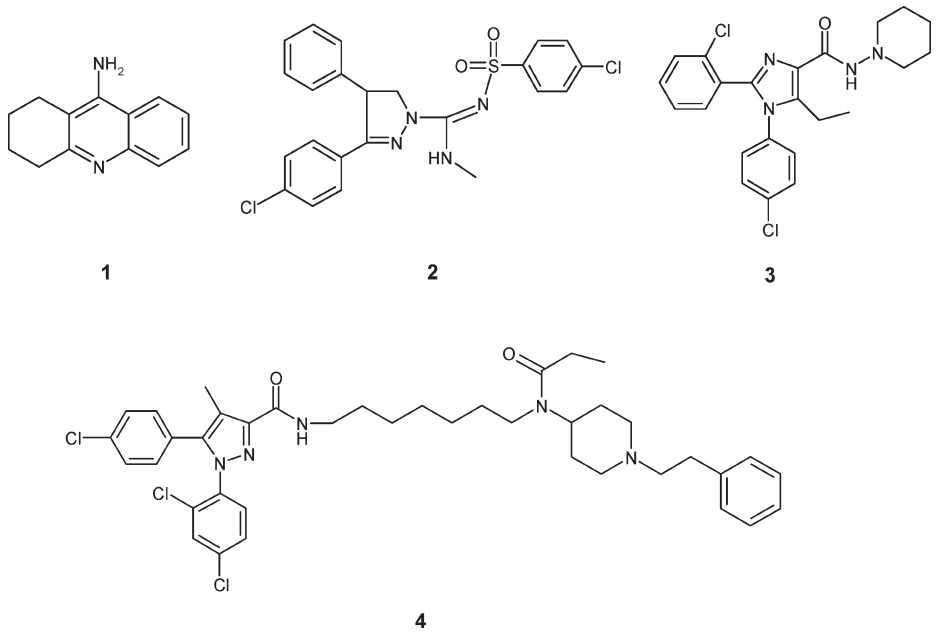

Figure 1. Chemical structures of the AChEI **1**, CB_1 receptor antagonists **2** and **3**, and Esteve's dual acting CB_1 receptor antagonist−μ-opioid receptor modulator **4**.

roles of CB_1 receptor antagonists as well as AChEIs in cognitive impairment.

In our design strategy, two molecular entities (interacting with high selectivity either to the CB_1 receptor or to the AChE enzyme) were applied as the starting points, thereby combining their key structural elements to incorporate activity at both targets into a single molecule. The 3,4-diarylpyrazoline[25] **2** and 1,2-diarylimidazole[27,28] **3** were selected as suitable CB_1 antagonistic structural elements[29] for this study (Figure 1), whereas **1** was preferred as a compact AChEI moiety. It was envisioned that connecting the CB_1 antagonistic units **2** and **3**, respectively, to **1** by an alkylene spacer of suitable length would result in dual acting AChEIs/CB_1 receptor antagonists. The choice of **2** and **3** enabled us to investigate the effect of the difference in sprouting of the tail connecting the tacrine moiety.

In the course of our investigations, researchers from Esteve patented[30] compound **4** and some derivatives with different alkylene spacer lengths as dual acting CB_1 receptor antagonists−μ-opioid receptor modulators. Compound **4** was claimed by Esteve to have moderate CB_1 receptor affinity (K_i = 701 nM) and μ-opioid receptor affinity (K_i = 6543 nM). It is interesting to note that **4** showed in vivo activities after intraperitoneal administration in CB_1 receptor as well as opioid receptor mediated models despite these observed moderate receptor affinities and its high molecular weight of 737. The reported[31] synergistic effect between CB_1 and μ-opioid receptor modulation may have a positive impact on the observed in vivo activities of **4**.

It was also envisioned that the tacrine moiety would be amenable for derivatization with preservation of AChE inhibiting ability, based on the reported structure of tacrine derivative **17** with the AChE enzyme[32] (Protein Data Bank (PDB) code 1UT6). The alkylene chain of **17** points toward the outer surface into an unoccupied region. The orientation of the tacrine skeleton is the same[33] as that in the structure of AChE with **1** based on X-ray diffraction data (PDB code 1ACJ). These observations corroborated our design hypothesis toward dual AChEI/CB_1 receptor antagonists.

Results and Discussion

The CB_1 receptor has a highly lipophilic binding site, and consequently CB_1 receptor agonists as well as antagonists generally are lipophilic entities which in general exhibit low aqueous solubilities. A poor water solubility may lead to practical difficulties in pharmacological testing and may necessitate the use of solubilizing agents and complex compound formulations. The compounds **5**−**10** were designed with the goal to produce CB_1 receptor antagonists with improved aqueous solubilities, due to the presence of either a polar group (**5** and **6**) or an ionizable nitrogen atom in their carboxamidine side chain (**7**−**10**).

Compounds **5**−**10** were synthesized in reasonable yields, ranging from 39% to 65%, by chlorinating the key intermediate[25] **11** with PCl_5 in chlorobenzene, followed by treatment with various amines (Scheme 1). Compound **7** was subsequently converted to the corresponding hydrochloric acid salt by treatment with 1 M HCl in ethanol.

The pharmacological results of the target compounds **5**−**10** and the reference compound **2** are given in Table 1. The CB_1 receptor binding data of **5**−**10** corroborated our hypothesis that the replacement of the amidine *N*-methyl group by larger and more polar groups leads to retained CB_1 receptor affinities. Compound **7** with the *N*,*N*-dimethylaminopropyl tail showed the highest CB_1 receptor affinity (3.1 nM) in this series. In general, the compounds **5**−**10** elicited high CB_1/CB_2 receptor selectivities, which is in line with the results from the reference compound **2**. It is interesting to note that the compounds **7**−**10**, which all have an ionizable nitrogen atom incorporated in their side chain, have approximately 10-fold lower CB_1 antagonistic potencies compared with the compounds **2** and **5**, **6** which are devoid of the presence of such an ionizable nitrogen atom. According to expectation, the compounds **7**−**10** exhibited improved aqueous solubilities as compared to **2** and **5**, **6**, in particular under acidic conditions (Table 1).

Our AChEI/CB_1 receptor antagonist combination design considerations led to the synthesis of the series based on **2**, targeting compounds **12** and **13** according to Scheme 2.

Scheme 1[a]

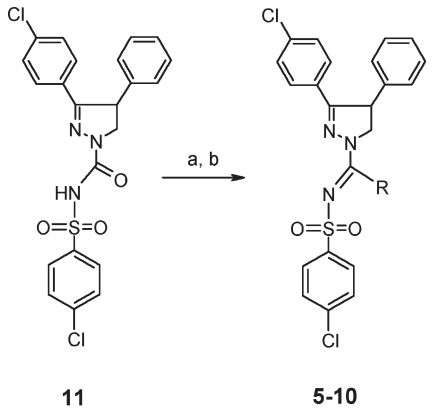

Compound	R	Yield (%)
5		50
6		59
7	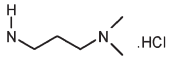	62
8	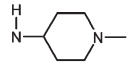	65
9	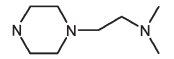	46
10	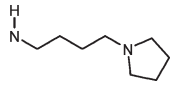	39

[a] Reagents and conditions: (a) PCl_5, chlorobenzene, reflux, 1 h; (b) RH, CH_2Cl_2, room temp, 16 h.

Table 1. In Vitro Pharmacological Results of Compounds **2** and **5**−**10**

compd	$K_i(CB_1)$,[a] nM	$pA_2(CB_1)$,[b]	$K_i(CB_2)$,[c] nM	aqueous solubility,[d] μM, (pH 2)	aqueous solubility,[e] μM, (pH 7.4)
2	25 ± 7	8.7 ± 0.3	> 1000	4	2
5	43 ± 11	9.0 ± 0.1	> 1000	4	4
6	31 ± 17	8.6 ± 0.2	571 ± 215	< 7	< 3
7	3.1 ± 0.9	7.8 ± 0.1	> 1000	> 100	38
8	19 ± 7	7.8 ± 0.1	> 1000	65	11
9	9.6 ± 1.4	7.6 ± 0.2	> 1000	65	4
10	27 ± 9	7.9 ± 0.2	> 1000	38	11

[a] Displacement of specific CP-55,940 binding in CHO cells stably transfected with human CB_1 receptor, expressed[25] as K_i ± SEM values (nM). [b] [^{3}H]Arachidonic acid release in CHO cells expressed[25] as pA_2 ± SEM values. [c] Displacement of specific CP-55,940 binding in CHO cells stably transfected with human CB_2 receptor, expressed[25] as K_i ± SEM values (nM). The values represent the mean result based on at least three independent experiments. [d] Turbidimetric aqueous solubility, pH 2. Estimated precipitation concentration expressed as μM. [e] Turbidimetric aqueous solubility, pH 7.4. Estimated precipitation concentration expressed as μM.

The chlorination reaction to convert **11** into its chloroimidoyl derivative **14** was carried out under milder reaction conditions (using a phosphorus oxychloride ($POCl_3$)/4-dimethylaminopyridine (DMAP) combination) compared to the synthesis of **5**−**10**. Subsequent reaction with the tacrine−alkylene spacer derivatives[34] **15** and **16** in the presence of Hünig's base furnished the target compounds **12** and **13** in 36% and 35% yield, respectively.

The synthesis of the **3**-based series, aiming at **20** and **21**, started with the hydrolysis of the ethyl ester precursor[27,28] **18**. Hydrolysis with LiOH in a water/THF mixture led to the corresponding carboxylic acid **19** in 84% yield. Subsequent amidation with the tacrine building blocks **15** and **16** in the presence of suitable coupling reagents led to the formation of the target compounds **20** and **21** in 53% and 62% yield, respectively (Scheme 3).

The pharmacological results of the target compounds **12**, **13**, **20**, and **21**, the reference compounds **1**−**3**, and the known CB_1 receptor antagonist rimonabant[35] are given in Table 2.

According to our expections, **1** was found inactive as CB_1 receptor ligand but active in the AChEI assay. In addition, both rimonabant and **3** are potent CB_1 receptor antagonists without significant AChE inhibiting properties. The target compounds **12**, **13**, **20**, **21** all showed significant CB_1 receptor affinities and in general acted as CB_1 receptor antagonists. The pyrazoline derivative **12** showed moderate AChE inhibiting properties, but compound **13** with a longer spacer length elicited a higher pIC_{50} value.

The imidazoles **20** and **21** showed also AChE inhibiting properties but in a reverse order. Compound **20** with the shorter spacer length is the more potent compound in this series, having AChE inhibitory activities comparable to those of the AChEI reference compound **1**.

In order to explain these observations, molecular modeling studies were performed on both the CB_1 receptor and the AChE enzyme. Several CB_1 receptor homology models have been reported in the literature.[25,36]

In the majority of these models the loop regions spanning the helices of the G-protein-coupled receptor (GPCR) have been omitted. We have rebuilt our model using the rigid template of the recently reported[37] human β_2-adrenergic structure and taking the extracellular loop 2 into account, including the cysteine bridge which is presumed to be present in the lipids GPCR cluster. After docking of **2**, all the essential features of the binding as reported earlier[25] were maintained including the key interaction between Lys192 and the sulfonamide moiety of **2** and the multiple $\pi-\pi$ stacking interactions of its pyrazoline aryl rings with a series of aromatic residues on the helices 5 and 6. The only difference with our previous model is a different orientation of the *p*-Cl-phenyl ring attached to the SO_2 group of **2**, which now points downward between the helices 3 and 6. The resulting conformation of **2**

Scheme 2[a]

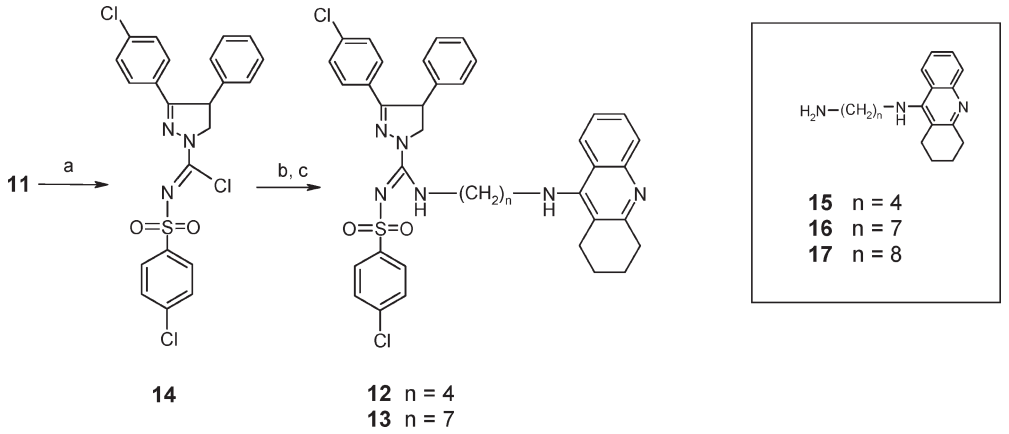

[a] Reagents and conditions: (a) $POCl_3$, DMAP, CH_2Cl_2, reflux, 5 h; (b) **15** or **16**, 0 °C; (c) Hünig's base, CH_2Cl_2, reflux, 72 h (35−36%).

Scheme 3[a]

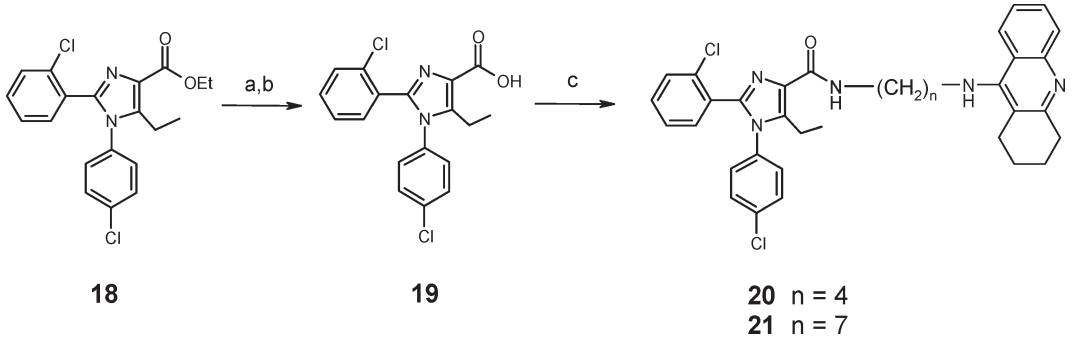

[a] Reagents and conditions: (a) LiOH, THF/H_2O, 70 °C, 16 h (84%); (b) concentrated HCl; (c) **15** or **16**, 1-hydroxy-7-azabenzotriazole (HOAt), 1-(3-dimethylaminopropyl)-3-ethylcarbodiimide·HCl (EDC), CH_2Cl_2, room temp, 72 h (53−62%).

Table 2. In Vitro Pharmacological Results of Rimonabant, Compounds **1**−**3**, **12**−**13**, **20**, **21**

compd	$K_i(CB_1)$,[a] nM	$pA_2(CB_1)$[b]	$K_i(CB_2)$,[c] nM	AChE inhibition (pIC_{50})[d]
rimonabant·HCl	25 ± 15 (11.5)[35]	8.6 ± 0.1	1580 ± 150 (1640)[35]	4.6 ± 0.2
tacrine (**1**)	> 1000	nd[e]	> 1000	6.6 ± 0.2
2	25 ± 7	8.7 ± 0.3	> 1000	nd[e]
3	14 ± 5	9.8 ± 0.2	> 1000	< 4.5
12	42 ± 13	8.1 ± 0.3	> 1000	5.6 ± 0.4
13	54 ± 14	7.4 ± 0.2	> 1000	6.0 ± 0.3
20	48 ± 27	nd[e]	> 1000	6.5 ± 0.3
21	88 ± 30	8.2[f]	> 1000	5.9 ± 0.3

[a] Displacement of specific CP-55,940 binding in CHO cells stably transfected with human CB_1 receptor, expressed as K_i ± SEM values (nM). [b] [^{3}H]Arachidonic acid release in CHO cells expressed as pA_2 ± SEM values. [c] Displacement of specific CP-55,940 binding in CHO cells stably transfected with human CB_2 receptor, expressed as K_i ± SEM values (nM). The values represent the mean result based on at least three independent experiments, unless indicated otherwise. [d] AChEI; human recombinant (HEK-293 cells); photometric detection; Cerep. [e] nd = not determined. [f] Result based on two independent experiments (8.2 and 8.2, respectively).

has a higher resemblance to our earlier reported X-ray structure of the 4*S*-enantiomer of **2**.[25]

In the loop region, positioned just above the CB_1 antagonist binding pocket, an additional pocket was recognized that can accommodate **1**. The docking result of **12** in the homology model of the CB_1 receptor is shown in Figure 2.

The protonated quinolinic nitrogen of **1** (ACD/pK_a = 9.2)[38] can interact with the Asp266 residue which also forms a salt bridge with Lys192. The aromatic ring of the tacrine part is postulated to stack between Phe177, Phe174, and His178. Its condensed cyclohexyl ring is enclosed by a small lipophilic pocket limited by Leu193 and Phe268. It is noted that the CB_1 pharmacophore part of **12** is positioned almost exactly as in the case of **2**.

The negative impact of linking a tacrine unit to the CB_1 antagonist pharmacophore on the binding and activity of **12**, **13**, **20**, and **21** is small, since they all still show CB_1 receptor affinity values in the nanomolar range. The reduction in CB_1 receptor affinities of the tacrine derivatives in the imidazole-based series (**20** and **21**) seems to be somewhat more pronounced (about 3- to 4-fold) than in the pyrazoline-based series (**12** and **13**) (~2-fold). This might be rationalized by the fact that in the former series one of the pharmacophoric features (the piperidinyl ring) is replaced by the linker while in the latter series the corresponding feature (the *p*-Cl-phenyl moiety), which is known to be important for CB_1 receptor interaction, is maintained.

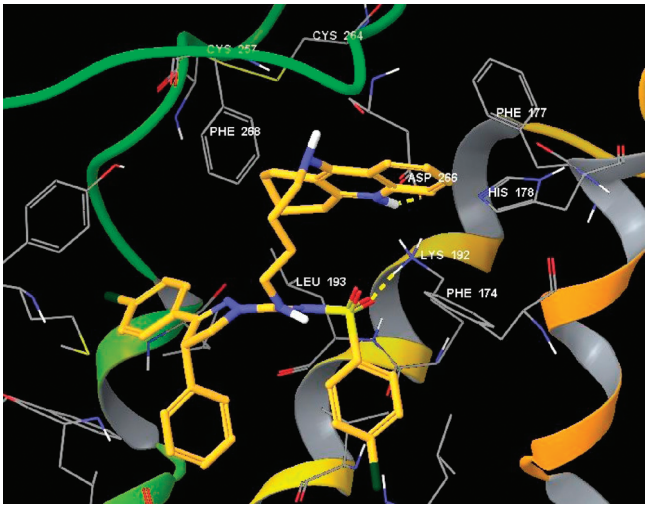

Figure 2. Docking result of **12** in the homology model of the CB_1 receptor. Helices 5 and 6 are not displayed for clarity.

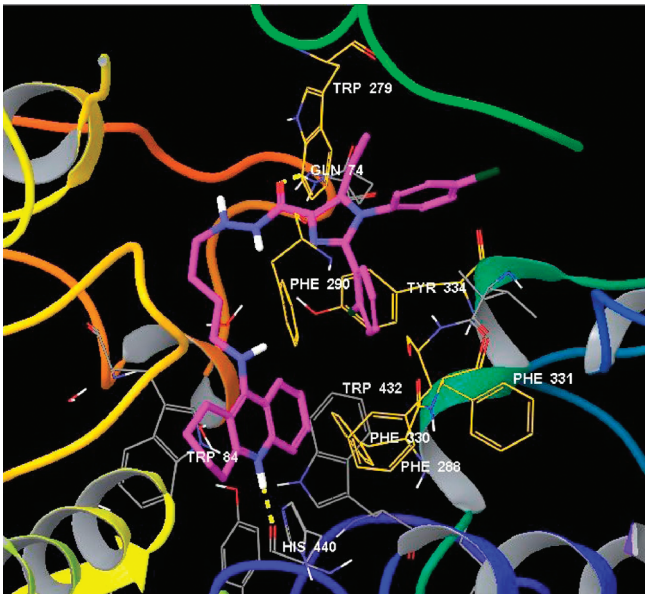

Figure 3. Docking result of **20** (shown in purple) in the structure of AChE. The lipophilic residues of the PAS accommodating the diaryl moiety of the CB_1 antagonistic part are given in orange. Some regions of the protein are not displayed for clarity.

The docking of **20** in AChE is depicted in Figure 3. The tacrine unit is found at the bottom of the active site gorge at exactly the same position of unlinked **1**, stacking between Trp84 and Phe330 as well as bound by a hydrogen bond with the backbone carbonyl group of His440. At the outer surface, at the so-called peripheral anionic site (PAS), there is a constitution of residues that accommodate the pyrazoline-based CB_1 pharmacophore surprisingly well (Figure 4).

The aromatic cluster Trp279, Phe288, Phe290, Phe330, and Phe331 can bind the aromatic rings of the CB_1 antagonists by multiple $\pi-\pi$ stacking interactions similar to the aromatic residues on helices 5 and 6 of the GPCR. The H-bonding to the sulfonamide of the **2** series and the corresponding amide of the **3** series can be realized by Gln74. The linking tail runs through the gorge following the trajectory of ACh on its way to the catalytic site.

According to the results in Table 2, the connection of the CB_1 antagonist part via the $n = 4$ alkylene spacer to the

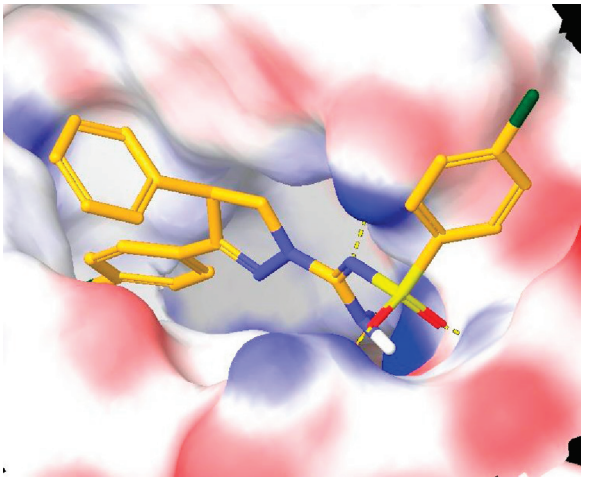

Figure 4. Docking result of the 3,4-diarylpyrazoline-based CB_1 pharmacophore in the structure of AChE.

Figure 5. Structure-based alignment of **12** and **20** showing the effect of the different sprouting of the tail from their CB_1 antagonist part.

tacrine moiety has a negative impact on the AChE inhibiting properties in the pyrazoline (**2**-based) series (compound **12**), whereas in the imidazole (**3**-based) series compound **20** is equipotent compared to **1**.

The distance between the anilinic nitrogen atom of **1** and the attachment nitrogen of docked **2** in the PAS is approximately 7.8 Å, while the same distance in the case of **3** is only 5.0 Å (Figure 5).

The latter can be bridged well by a C_4 chain (6.3 Å) which results in **20**, while in the former case the C_4 chain connection, resulting in **12**, will prevent an optimal fit into the AChE structure. This further illustrates that the different modes of attachment of the tacrine-spacer unit to the CB_1 antagonist pharmacophore in compounds **12** and **20**, respectively, have an impact on the optimal spacer lengths.[29]

Finally, two additional points are of interest. First, the AChEI **1** and some of its metabolites have been reported[39] to elicit toxic effects. In this regard our compounds **12**, **13**, **20**, and **21** might be expected to elicit some of the adverse effects

of **1**. However, it is realized that *N*,*N*′-bis(1,2,3,4-tetrahydroacridin-9-yl)heptane-1,7-diamine (bis(7)-tacrine) demonstrated[40] a minor toxicity in comparison with **1** and accordingly the tacrine heterodimers **12**, **13**, **20**, and **21** would be anticipated to be considerably less toxic than **1**. Second, although the more general term "antagonist" is used in this article, it is with the understanding that the majority of the reported cannabinoid CB_1 receptor antagonists[29,41] (including compounds such as rimonabant, **2**, and **3**) behave as inverse agonists[42] at the constitutively active[43] CB_1 GPCR. Therefore, it can be anticipated that the compounds **5**−**10**, **12**, **13**, **20**, and **21** will also act as inverse agonists at the CB_1 receptor.

Conclusion

Novel hybrid molecules **12**, **13**, **20**, **21** exhibiting AChE inhibiting activities as well as significant cannabinoid CB_1 receptor antagonistic properties were discovered that are based on **1** as the AChEI pharmacophore and known cannabinoid CB_1 antagonistic counterparts. The imidazole-based **20** showed significant CB_1 receptor affinity (48 nM) in combination with high CB_1/CB_2 receptor subtype selectivity (> 20-fold) and elicited equipotent AChE inhibitory activity compared with **1**.

Experimental Section

Chemistry. ^{1}H and ^{13}C NMR spectra were recorded on a Varian UN400 instrument (400 MHz) using $CDCl_3$ as solvent with tetramethylsilane as an internal standard. Chemical shifts are given in parts per million (ppm) (δ scale) downfield from tetramethylsilane. Coupling constants (*J*) are expressed in hertz (Hz). Thin-layer chromatography was performed on Merck precoated 60 F_{254} plates, and spots were visualized with UV light. Flash chromatography was performed using silica gel 60 (0.040−0.063 mm, Merck). Column chromatography was performed using silica gel 60 (0.063−0.200 mm, Merck). Melting points were recorded on a Büchi B-545 melting point apparatus and are uncorrected. Mass spectra were recorded on a Micromass QTOF-2 instrument with MassLynx application software for acquisition and reconstruction of the data. Exact mass measurement by HRMS was done of the quasimolecular ion $[M + H]^+$. Elemental analyses were performed on a Vario EL elemental analyzer by Solvay Pharmaceuticals. Yields refer to isolated pure products and were not maximized. The purity of the target compounds **3**, **5**−**10**, **12**, **13**, **20**, and **21** was established as ≥95%, based on combustion analysis data.

1-(4-Chlorophenyl)-2-(2-chlorophenyl)-5-ethyl-*N*-(piperidin-1-yl)-1*H*-imidazole-4-carboxamide·$^2/_3$H$_2$O (3). Compound **3** was obtained from **19** according to reported procedures.[27,28] Mp: 207−208 °C. ^{1}H NMR (400 MHz, $CDCl_3$) δ 1.08 (t, *J* = 7.5 Hz, 3H), 1.39−1.48 (m, 2H), 1.69−1.81 (m, 5H), 2.86 (br s, 3H), 2.94 (q, *J* = 7.5 Hz, 2H), 7.09 (d, *J* = 8.7 Hz, 2H), 7.20−7.38 (m, 6H), 7.94 (s, 1H). ^{13}C NMR (100 MHz, $CDCl_3$) δ 13.9, 17.7, 23.4, 25.5, 57.3, 126.7, 129.0, 129.4, 129.7, 129.8, 130.0, 131.0, 132.5, 133.8, 134.5, 135.1, 140.3, 143.2, 160.5. HRMS ($C_{23}H_{25}Cl_2N_4O$) $[M + H]^+$: found *m*/*z* 443.1413, calcd 443.1405. Anal. ($C_{23}H_{24}Cl_2N_4O$) C, H, N.

3-(4-Chlorophenyl)-*N*′-((4-chlorophenyl)sulfonyl)-*N*-(2-hydroxy-2-methylpropyl)-4-phenyl-4,5-dihydro-1*H*-pyrazole-1-carboxamidine (5). Compound **5** was obtained from **11** and 1-amino-2-methylpropan-2-ol according to the procedure described for **7**. Mp: 154−155 °C. ^{1}H NMR (400 MHz, $CDCl_3$) δ 1.30 (s, 3H), 1.31 (s, 3H), 1.63 (br s, 1H), 2.30 (br s, 1H), 3.63−3.71 (m, 2H), 4.07 (dd, *J* = 11.6 and 5.5 Hz, 1H), 4.52 (t, *J* = 11.6 Hz, 1H), 4.66 (dd, *J* = 11.6 and 5.5 Hz, 1H), 7.12 (d, *J* = 6.6 Hz, 2H), 7.23−7.34 (m, 5H), 7.37 (d, *J* = 8.8 Hz, 2H), 7.51 (d, *J* = 8.8 Hz, 2H), 7.86 (d, *J* = 8.6 Hz, 2H). ^{13}C NMR (100 MHz, $CDCl_3$) δ 27.42, 27.45, 50.9, 54.8, 57.4, 70.5, 127.3, 127.4, 128.1, 128.4, 128.6, 128.7, 129.0, 129.5, 136.6, 137.4, 139.1, 143.3, 152.2, 157.5. HRMS ($C_{26}H_{27}Cl_2N_4O_3S$) $[M + H]^+$: found *m*/*z* 545.1188, calcd 545.1181. Anal. ($C_{26}H_{26}Cl_2N_4O_3S$) C, H, N.

[3-(4-Chlorophenyl)-4-phenyl-4,5-dihydro-1*H*-pyrazol-1-yl]-[4-(1,1-dioxothiomorpholinyl)methylene]-4-chlorobenzenesulfonamide (6). Compound **6** was obtained from **11** and thiomorpholine 1,1-dioxide according to the procedure described for **7**. ^{1}H NMR (400 MHz, $CDCl_3$) δ 3.28−3.46 (m, 4H), 3.80 (dd, *J* = 11 and 5 Hz, 1H), 4.18−4.24 (m, 4H), 4.39 (t, *J* = 11 Hz, 1H), 4.62 (dd, *J* = 11 and 5 Hz, 1H), 7.07−7.12 (m, 2H), 7.26−7.36 (m, 5H), 7.39 (d, *J* = 9 Hz, 2H), 7.48 (d, *J* = 9 Hz, 2H), 7.82 (d, *J* = 9 Hz, 2H). HRMS ($C_{26}H_{25}Cl_2N_4O_4S_2$) $[M + H]^+$: found *m*/*z* 591.0707, calcd 591.0694. Anal. ($C_{26}H_{24}Cl_2N_4O_4S_2$) C, H, N.

3-(4-Chlorophenyl)-*N*′-((4-chlorophenyl)sulfonyl)-*N*-[3-(dimethylamino)propyl]-4-phenyl-4,5-dihydro-1*H*-pyrazole-1-carboxamidine·HCl (7). A magnetically stirred mixture of **11**[25] (2.37 g, 5.0 mmol) and PCl_5 (1.05 g, 5.0 mmol) in chlorobenzene (50 mL) was heated at reflux temperature for 1 h. After thorough concentration, the formed **13** was suspended in CH_2Cl_2 and reacted with excess cold 3-(dimethylamino)propylamine (2.55 g, 25 mmol). After being stirred at room temperature for 16 h, the mixture was washed with water, dried over $MgSO_4$, filtered, and concentrated in vacuo. Flash chromatographic purification (eluant ethyl acetate/methanol = 1/2 (v/v)) gave pure 3-(4-chlorophenyl)-*N*′-[(4-chlorophenyl)sulfonyl]-*N*-[3-(dimethylamino)-propyl]-4-phenyl-4,5-dihydro-1*H*-pyrazole-1-carboxamidine **7** as its free base: ^{1}H NMR (400 MHz, $CDCl_3$) δ 1.77 (quint, *J* = 6 Hz, 2H), 2.29 (s, 6H), 2.48 (t, *J* = 6.2 Hz, 2H), 3.70 (q, *J* = 5.6 Hz, 2H), 4.10 (dd, *J* = 11.3 and 5.2 Hz, 1H), 4.53 (t, *J* = 11.4 Hz, 1H), 4.61−4.68 (m, 1H), 7.10−7.14 (m, 2H), 7.22−7.33 (m, 5H), 7.36 (d, *J* = 8.8 Hz, 2H), 7.52 (d, *J* = 8.8 Hz, 2H), 7.85 (d, *J* = 8.8 Hz, 2H), 8.62 (br s, 1H). Subsequent treatment with 1 M HCl/EtOH (5 mL) and trituration with diethyl ether gave the corresponding hydrochloric acid salt as a white solid (1.83 g, 62% yield). Mp: 236−237 °C. ^{1}H NMR (400 MHz, $CDCl_3$) δ 1.65 (br s, ∼1H), 2.26 (quint, *J* = 7 Hz, 2H), 2.80 (s, 6H), 3.05−3.17 (m, 2H), 3.74−3.82 (m, 2H), 4.11 (dd, *J* = 11 and 5 Hz, 1H), 4.56 (t, *J* = 11 Hz, 1H), 4.71 (dd, *J* = 11 and 5 Hz, 1H), 7.14 (br d, *J* = 8 Hz, 2H), 7.21−7.35 (m, 5H), 7.39 (br d, *J* = 8 Hz, 2H), 7.61−7.67 (m, 3H), 7.85 (br d, *J* = 8 Hz, 2H). ^{13}C NMR (100 MHz, $CDCl_3$) δ 25.0, 40.6, 43.0, 51.3, 55.1, 57.5, 127.2. 127.4, 128.1, 128.2, 128.8, 129.0, 129.1, 129.5, 136.7, 137.4, 139.0, 143.7, 151.4, 158.0. HRMS ($C_{27}H_{30}Cl_2N_5O_2S$) $[M + H]^+$: found *m*/*z* 558.1513, calcd 558.1497. Anal. ($C_{26}H_{30}Cl_2N_5O_2S\cdot HCl$) C, H, N.

3-(4-Chlorophenyl)-*N*′-((4-chlorophenyl)sulfonyl)-*N*-[4-(methyl)-piperidin-4-yl]-4-phenyl-4,5-dihydro-1*H*-pyrazole-1-carboxamidine (8). Compound **8** was obtained from **11** and 1-methylpiperidin-4-ylamine according to the procedure described for **7**. Mp: 202−203 °C. ^{1}H NMR (400 MHz, $CDCl_3$) δ 1.58−1.74 (m, 3 H), 1.97−2.17 (m, 4H), 2.31 (s, 3H), 2.74−2.84 (m, 2H), 3.98−4.22 (m, 2H), 4.49−4.71 (m, 2H), 7.11 (d, *J* = 6.6 Hz, 2H), 7.23−7.35 (m, 5H), 7.39 (d, *J* = 8.6 Hz, 2H), 7.49 (d, *J* = 8.6 Hz, 2H), 7.84 (d, *J* = 8.6 Hz, 2H). HRMS ($C_{28}H_{30}Cl_2N_5O_2S$) $[M + H]^+$: found *m*/*z* 570.1497, calcd 570.1497. Anal. ($C_{28}H_{29}Cl_2N_5O_2S$) C, H, N.

[3-(4-Chlorophenyl)-4-phenyl-4,5-dihydro-1*H*-pyrazol-1-yl]-{[2-(dimethylamino)ethylpiperazin-4-yl]methylene}-4-chlorobenzenesulfonamide·$^1/_4$H$_2$O (9). Compound **9** was obtained from **11** and dimethyl(2-piperazin-1-ylethyl)amine according to the procedure described for **7**. Mp: 164−165 °C. ^{1}H NMR (400 MHz, $CDCl_3$) δ 2.30 (s, 6H), 2.50 (t, *J* = 6.5 Hz, 2H), 2.57−2.62 (m, 2H), 2.64−2.78 (m, 4H), 3.72−3.89 (m, 5H), 4.42 (t, *J* = 11.2 Hz, 1H), 4.52−4.58 (m, 1H), 7.11 (br d, *J* = 8 Hz, 2H), 7.23−7.34 (m, 5H), 7.36 (d, *J* = 8.6 Hz, 2H), 7.49 (d, *J* = 8.8 Hz, 2H), 7.83 (d, *J* = 8.8 Hz, 2H). ^{13}C NMR (100 MHz, $CDCl_3$) δ 45.8, 50.0, 50.1, 53.4, 56.4, 56.8, 58.2, 127.1, 127.3, 128.0, 128.5, 128.70, 128.74, 129.0, 129.5, 136.4, 137.1, 139.1, 144.1, 153.0, 157.2. HRMS ($C_{30}H_{35}Cl_2N_6O_2S$) $[M + H]^+$: found *m*/*z* 613.1932, calcd 613.1919. Anal. ($C_{30}H_{34}Cl_2N_6O_2S$) C, H, N.

3-(4-Chlorophenyl)-*N*′-((4-chlorophenyl)sulfonyl)-*N*-[4-(pyrrolidin-1-yl)butyl]-4-phenyl-4,5-dihydro-1*H*-pyrazole-1-carboxamidine (10). Compound **10** was obtained from **11** and 4-(pyrrolidin-1-yl)-butylamine according to the procedure described for **7**. Mp: 126−127 °C. ^{1}H NMR (400 MHz, $CDCl_3$) δ 1.56−1.65 (m, 2H), 1.65−1.75 (m, 3H), 1.75−1.81 (m, 4H), 2.44−2.54 (m, 6H), 3.59−3.67 (m, 2H), 4.12 (dd, J = 11.3 and 4.7 Hz, 1H), 4.55 (t, J = 11.5 Hz, 1H), 4.61 −4.67 (m, 1H), 7.10−7.14 (m, 2H), 7.23−7.34 (m, 5H), 7.38 (d, J = 8.8 Hz, 2H), 7.50 (d, J = 8.8 Hz, 2H), 7.85 (d, J = 8.8 Hz, 2H). ^{13}C NMR (100 MHz, $CDCl_3$) δ 23.4, 26.2, 28.2, 44.9, 50.6, 54.2, 55.9, 57.7, 127.3, 127.4, 128.0, 128.5, 128.6, 128.7, 129.0, 129.5, 136.5, 137.3, 139.1, 143.3, 151.9, 157.4. HRMS ($C_{30}H_{34}Cl_2N_5O_2S$) $[M + H]^+$: found m/z 598.1824, calcd 598.1810. Anal. ($C_{30}H_{33}Cl_2N_5O_2S$) C, H, N.

4-Chloro-*N*-{[3-(4-chlorophenyl)-4-phenyl-4,5-dihydro-1*H*-pyrazolyl][4-(1,2,3,4-tetrahydroacridin-9-ylamino)butylamino]methylene}benzenesulfonamide·2H$_2$O·1.5MeOH (12). Compound **12** was obtained from **11** and **15** according to the procedure described for **13**. Mp: 125−126 °C. ^{1}H NMR (400 MHz, $CDCl_3$) δ 1.80−2.01 (m, 8H), 2.60−2.70 (m, 2H), 3.25−3.34 (m, 2H), 3.77−3.86 (m, 2H), 3.95−4.06 (m, 3H), 4.43 (t, J = 12 Hz, 1H), 4.67 (dd, J = 12 and 5 Hz, 1H), 6.30 (br s, 1H), 7.10 (br d, J = 8 Hz, 2H), 7.15−7.31 (m, 6H), 7.36−7.44 (m, 3H), 7.52 (d, J = 8 Hz, 2H), 7.65 (t, J = 8 Hz, 1H), 7.83 (d, J = 8 Hz, 2H), 8.20 (d, J = 8 Hz, 1H), 8.52 (d, J = 8 Hz, 1H). ^{13}C NMR (100 MHz, $CDCl_3$) δ 20.6, 22.0, 24.1, 27.1, 27.9, 28.6, 43.9, 47.2, 50.8, 57.3, 111.3, 115.9, 120.8, 124.3, 125.1, 127.1, 127.3, 128.1, 128.3, 128.76, 128.80, 129.0, 129.5, 132.1, 136.6, 137.5, 138.8, 139.0, 143.3, 151.4, 151.6, 155.6, 157.7. HRMS ($C_{39}H_{39}Cl_2N_6O_2S$) $[M + H]^+$: found m/z 725.2255, calcd 725.2232. Anal. ($C_{39}H_{38}Cl_2N_6O_2S$) C, H, N.

4-Chloro-*N*-{[3-(4-chlorophenyl)-4-phenyl-4,5-dihydro-1*H*-pyrazolyl]-[7-(1,2,3,4-tetrahydroacridin-9-ylamino)heptylamino]-methylene}benzenesulfonamide·$^3/_4$H$_2$O (13). To a magnetically stirred solution of **11**[25] (1.5 g, 3.16 mmol) in dichloromethane were successively added (30 mL) DMAP (1.707 g, 13.9 mmol) and $POCl_3$ (0.59 g, 3.85 mmol), and the resulting magnetically stirred mixture was heated at reflux temperature for 5 h. The resulting mixture was allowed to attain room temperature and concentrated in vacuo to give crude **14**, which was dissolved in dichloromethane (30 mL) and reacted at 0 °C with *N*-[9′-(1′,2′,3′,4′-tetrahydroacridinyl)]-1,7-diaminoheptane **16** (1.48 g, 4.75 mmol). After addition of *N*,*N*-diisopropylethylamine (DIPEA) (1.02 g, 7.9 mmol) the reaction mixture was heated at reflux temperature for 72 h. The resulting mixture was allowed to attain room temperature and was washed with water and brine successively, dried over Na_2SO_4, filtered, and concentrated. The obtained crude product was purified by flash chromatography (gradient, dichloromethane → dichloromethane/methanol = 95/5 (v/v)) to give pure **13** (0.85 g, 35% yield). Mp: 90−91 °C. ^{1}H NMR (400 MHz, $CDCl_3$) δ 1.20−1.73 (m, 10H), 1.86−1.96 (m, 4H), 2.66−2.74 (m, 2H), 3.05−3.12 (m, 2H), 3.47−3.56 (m, 2H), 3.58−3.67 (m, 2H), 4.07−4.14 (m, 1H), 4.52 (t, J = 12 Hz, 1H), 4.58−4.66 (m, 1H), 7.11 (br d, J = 8 Hz, 2H), 7.21−7.40 (m, 8H), 7.49 (br d, J = 8 Hz, 2H), 7.56 (br t, J = 8 Hz, 1H, 7.83 (br d, J = 8 Hz, 2H), 7.93−8.00 (m, 2H). HRMS ($C_{42}H_{45}Cl_2N_6O_2S$) $[M + H]^+$: found m/z 767.2734, calcd 767.2702. Anal. ($C_{42}H_{44}Cl_2N_6O_2S$) C, H, N.

2-(2-Chlorophenyl)-1-(4-chlorophenyl)-5-ethyl-1*H*-imidazole-4-carboxylic Acid (19). To a magnetically stirred solution of **18**[27] (5.80 g, 0.0149 mol) in tetrahydrofuran (40 mL) was added a solution of LiOH (0.715 g) in water (40 mL). The resulting mixture was heated at 70 °C for 16 h. The resulting mixture was allowed to attain room temperature and subsequently treated with concentrated hydrochloric acid (3.5 mL). The tetrahydrofuran was evaporated in vacuo, and the resulting mixture was stirred overnight. The formed precipitate was collected by filtration and washed with petroleum ether (40−60) to give **19** (4.52 g, 84% yield). ^{1}H NMR (400 MHz, $CDCl_3$): δ 1.09 (t, J = 7, 3H), 2.90 (q, J = 7, 2H), 3.70 (br s, 1H), 7.12 (dt, J = 8 and 2, 2H), 7.22−7.28 (m, 1H), 7.29−7.38 (m, 5H).

***N*-[4-(1,2,3,4-Tetrahydroacridin-9-ylamino)butyl]-2-(2-chlorophenyl)-1-(4-chlorophenyl)-5-ethyl-1*H*-imidazole-4-carboxamide·H$_2$O (20).** Compound **20** was obtained from **15** and **19** according to the procedure described for **21**. Mp: 179−180 °C. ^{1}H NMR (400 MHz, $CDCl_3$) δ 1.06 (t, J = 7 Hz, 3H), 1.40−1.52 (m, 6H), 1.55−1.68 (m, 2H), 1.80−2.02 (m, 6H), 2.60 (t, J = 6 Hz, 2H), 2.95 (q, J = 7 Hz, 2H), 3.35 (t, J = 6 Hz, 2H), 3.42 (q, J = 7 Hz, 2H), 3.91 (br s, 2H), 5.60 (br s, 1H), 7.09 (d, J = 8 Hz, 2H), 7.20−7.36 (m, 6H), 7.45 (t, J = 7 Hz, 1H), 7.70 (t, J = 7 Hz, 2H), 8.17 (d, J = 8 Hz, 1H), 8.60 (br d, J = 7 Hz, 1H). HRMS ($C_{35}H_{36}Cl_2N_5O$) $[M + H]^+$: found m/z 612.2300, calcd 612.2297. Anal. ($C_{35}H_{35}Cl_2N_5O$) C, H, N.

***N*-[7-(1,2,3,4-Tetrahydroacridin-9-ylamino)heptyl]-2-(2-chlorophenyl)-1-(4-chlorophenyl)-5-ethyl-1*H*-imidazole-4-carboxamide·1.5H$_2$O·2MeOH (21).** To a magnetically stirred solution of *N*-[9′-(1′,2′,3′,4′-tetrahydroacridinyl)]-1,7-diaminoheptane **16** (0.837 g, 3.11 mmol) in dichloromethane (40 mL) was successively added **19** (0.75 g, 2.08 mmol), HOAt (0.34 g, 2.5 mmol), and EDC (0.48 g, 2.5 mmol). The resulting mixture was stirred at room temperature for 18 h and successively washed with water (2 × 50 mL) and brine (50 mL). The organic layer was successively dried over Na_2SO_4, filtered, and concentrated in vacuo. The obtained crude product was purified by flash chromatography (gradient, dichloromethane/ethanol = 99/1 → dichloromethane/ methanol = 90/10 (v/v)) to give pure **21** (780 mg, 62% yield). Mp: 110−111 °C. ^{1}H NMR (400 MHz, $CDCl_3$) δ 1.07 (t, J = 7 Hz, 3H), 1.67−1.85 (m, 4H), 1.88−1.99 (m, 4H), 2.68−2.78 (m, 2H), 2.95 (q, J = 7 Hz, 2H), 3.06−3.15 (m, 2H), 3.45−3.63 (m, 4H), 7.10 (br d, J = 8 Hz, 2H), 7.20−7.41 (m, 9H), 7.52−7.62 (m, 1H), 7.92−8.05 (m, 2H). HRMS ($C_{38}H_{42}Cl_2N_5O$) $[M + H]^+$: found m/z 654.2773, calcd 654.2766. Anal. ($C_{38}H_{41}Cl_2N_5O$) C, H, N.

Turbidimetric Aqueous Solubility Assay. Four dilutions of the test compound (10 mM in DMSO) were prepared in DMSO (3, 1, 0.3, and 0.1 mM). Each test compound concentration was then further diluted 1 in 100 in buffer (typically 0.01 M phosphate buffered saline, pH 7.4, or a buffer at pH 2) so that the final DMSO concentration was 1% and the final test compound concentrations were 1, 3, 10, 30, and 100 μM. The experiment was performed at 37 °C, and seven replicate wells were designated per concentration. Following the addition of the DMSO dilution to the buffer, the plates were incubated for 2 h at 37 °C before the absorbance was measured at 620 nm. The solubility was estimated from the concentration of test compound that produced an increase in absorbance above vehicle control (i.e., 1 % DMSO in buffer). Nicardipine and pyrene were included as control compounds. The solubility of nicardipine was pH dependent, whereas the solubility of pyrene was pH independent. Results were given as a calculated midrange value, based on measured lower and upper bound values.

Inhibition of AChE in Human HEK-293 Cells.[44] Test compounds were dissolved in DMSO (10 mM) and diluted to test concentrations in assay buffer. Testing was performed at a 3 log concentration range around a predetermined IC_{50} for the respective assay: e.g., 10, 1, 0.1, and 0.01 μM for IC_{50} of 0.3 μM and 300, 30, 3, and 0.3 nM for IC_{50} of 10 nM. All determinations were performed as duplicates. The highest concentration tested for primes was 10 μM. Following incubation of test compound with an AChE enzyme preparation (human recombinant expressed in HEK-293 cells) and the substrate acetylthiocholine (50 μM) for 30 min at 37 °C, the thio conjugate product was determined by photometry. Results were expressed as percentage of total product formed at each concentration of compound tested (duplicates). From the concentration−production inhibition curves, IC_{50} values were determined by nonlinear regression analysis using Hill equation curve fitting. Results were expressed as pIC_{50} values. Compounds with no significant affinity at concentrations of 10 μM and higher were considered inactive: $pIC_{50} < 5.0$.

Molecular Modeling. Modeling studies were performed using Schrödinger software (*Maestro*, version 8.5; Schrödinger LLC: New York, **2009**). The cannabinoid CB_1 receptor homology model was built with Prime using the X-ray structure of the β_2-adrenergic receptor (PDB code 2RH1) as rigid template. The extracellular loop 2 was modeled with the loop prediction module. The loop was modified in order to make the Cys bridge between C257 and C264 possible via a stepwise decreasing distance constraint minimization and after building the bridge, a full minimization of the loop. The tacrine moiety was docked in the described region manually without any further modifications.

The X-ray structure of AChE was processed with the Protein Preparation Wizard in Maestro. The CB_1 receptor binding site was disclosed by adjusting the rotameric state of two lipophilic residues (Phe331 $g^+ \rightarrow g^-$, Phe330 trans $\rightarrow g^-$). The CB_1 receptor antagonist moieties of **12**, **13**, **20**, and **21** were docked manually into this site with the tacrine part kept in the same position as that in its X-ray structure with AChE (PDB code 1ACJ).

Acknowledgment. Hugo Morren is gratefully acknowledged for supply of the high resolution mass spectrometry (HRMS) data. Peter Pfaffenbach is gratefully acknowledged for supply of the combustion analysis data. Pieter Spaans is acknowledged for supply of the turbidimetric aqueous solubility data. Mercachem B.V. (The Netherlands) is acknowledged for the synthesis of compounds **12**, **13**, **20**, and **21**.

References

(1) (a) Terry, A. V.; Buccafusco, J. J. The cholinergic hypothesis of age and Alzheimer's disease-related cognitive deficits: recent challenges and their implications for novel drug development. *J. Pharmacol. Exp. Ther*. **2003**, *306*, 821–827. (b) Sorbera, L. A.; Bozzo, J.; Serradell, N. Alzheimer's disease one century later: the search for effective targets continues. *Drugs Future* **2007**, *32*, 625–641.

(2) (a) Brufani, M.; Filocamo, L.; Lappa, S.; Maggi, A. New acetyl cholinesterase inhibitors. *Drugs Future* **1997**, *22*, 397–410. (b) Weinstock, M. Selectivity of cholinesterase inhibition, clinical implications for the treatment of Alzheimer's disease. *CNS Drugs* **1999**, *12*, 307–323.

(3) (a) Tumiatti, V.; Bolognesi, M. L.; Minarini, A; Rosini, M.; Milelli, A.; Matera, R.; Melchiorre, C. Progress in acetylcholinesterase inhibitors for Alzheimer's disease: an update. *Expert Opin. Ther. Pat*. **2008**, *18*, 387–401. (b) Marco, J. L.; Carreiras, M. C. Recent developments in the synthesis of acetylcholinesterase inhibitors. *Mini-Rev. Med. Chem*. **2003**, *3*, 518–524.

(4) Spencer, C. M.; Noble, S. Rivastigmine. A review of its use in Alzheimer's disease. *Drugs Aging* **1998**, *13*, 391–411.

(5) McKeith, I.; Del Ser, T.; Spano, P.; Emre, M.; Wesnes, K.; Anand, R.; Cicin-Sain, A.; Ferrara, R.; Spiegel, R. Efficacy of rivastigmine in dementia with Lewy bodies: a randomised, double-blind, placebo-controlled international study. *Lancet* **2000**, *356*, 2031–2036.

(6) Werber, E. A.; Rabey, J. M. The beneficial effect of cholinesterase inhibitors on patients suffering from Parkinson's disease and dementia. *J. Neural Transm*. **2001**, *108*, 1319–1325.

(7) Kumar, V.; Anand, R.; Messina, J.; Hartma, R.; Veach, J. An efficacy and safety analysis of Exelon in Alzheimer's disease patients with concurrent vascular risk factors. *Eur. J. Neurol*. **2000**, *7*, 159–169.

(8) Masanic, C. A.; Bayey, M. T.; van Reekum, R.; Simard, M. Open-label study of donepezil in traumatic brain injury. *Arch. Phys. Med. Rehabil*. **2001**, *82*, 896–901.

(9) Porcel, J.; Montalban, X. Anticholinesterasics in the treatment of cognitive impairment in multiple sclerosis. *J. Neurol. Sci*. **2006**, *245*, 177–181.

(10) (a) Castellano, C.; Rossi-Arnaud, C.; Cestari, V.; Costanzi, M. Cannabinoids and memory: animal studies. *Curr. Drug Targets: CNS Neurol. Disorders* **2003**, *2*, 389–402. (b) Wolff, M. C.; Leander, J. D. SR141716A, a cannabinoid CB_1 receptor antagonist improves memory in a delayed radial maze task. *Eur. J. Pharmacol*. **2003**, *477*, 213–217.

(11) De Groot, A.; Köfalvi, A; Wade, M. R.; Davis, R. J.; Rodrigues, R. J.; Rebola, N.; Cunha, R. A.; Nomikos, C. G. CB_1 receptor antagonism increases hippocampal acetylcholine release: site and mechanism of action. *Mol. Pharmacol*. **2006**, *70*, 1236–1245.

(12) Wise, L. E.; Iredale, P. A.; Stokes, R. J.; Lichtman, A. H. Combination of rimonabant and donezepil prolongs spatial memory duration. *Neuropsychopharmacology* **2007**, *32*, 1805–1812.

(13) Hikida, T.; Kitabatake, Y.; Pastan, I.; Nakanishi, S. Acetylcholine enhancement in the nucleus accumbens prevents addictive behaviors of cocaine and morphine. *Proc. Natl. Acad. Sci. U.S.A*. **2003**, *100*, 6169–6173.

(14) (a) Cohen, C.; Perrault, G.; Voltz, C; Steinberg, R.; Soubrié, P. SR141716, a central cannabinoid (CB_1) receptor antagonist, blocks the motivational and dopamine releasing effects of nicotine in rats. *Behav. Pharmacol*. **2002**, *13*, 451–463. (b) Solinas, M.; Paulilio, L. V.; Antoniou, K.; Pappas, L. A.; Goldberg, S. R. The cannabinoid CB1 antagonist N-piperidinyl-5-(4-chlorophenyl)-1-(2,4-dichlorophenyl)-4-methylpyrazole-3-carboxamide (SR-141716A) differentially alters the reinforcing effects of heroin under continuous reinforcement, fixed ratio, and progressive ratio schedules of drug self-administration in rats. *J. Pharmacol. Exp. Ther*. **2003**, *306*, 93–102.

(15) (a) Cavalli, A.; Bolognesi, M. L.; Minarini, A.; Rosini, M.; Tumiatti, V.; Recanatini, M.; Melchiorre, C. Multi-target-directed ligands to combat neurodegenerative diseases. *J. Med. Chem*. **2008**, *51*, 347–372. (b) Zimmermann, G. R.; Léhar, J.; Keith, C. T. Multi-target therapeutics: when the whole is greater than the sum of the parts. *Drug Discovery Today* **2007**, *12*, 34–42. (c) Morphy, R.; Rankovic, Z. The physicochemical challenges of designing multiple ligands. *J. Med. Chem*. **2006**, *49*, 4961–4970. (d) Van der Schyf, C. J.; Geldenhuys, W. J.; Youdim, M. B. H. Multifunctional neuroprotective drugs for the treatment of cognitive and movement impairment disorders, including Alzheimer's and Parkinson's diseases. *Drugs Future* **2006**, *31*, 447–460. (e) Morphy, R.; Rankovic, Z. Designed multiple ligands. An emerging drug discovery paradigm. *J. Med. Chem*. **2005**, *48*, 6523–6543.

(16) Bembenek, S. D.; Keith, J. M.; Letavic, M. A.; Apodaca, R.; Barbier, A. J.; Dvorak, L.; Aluisio, L.; Miller, K. L.; Lovenberg, T. W.; Carruthers, N. I. Lead identification of acetylcholinesterase inhibitors-histamine H_3 receptor antagonists from molecular modeling. *Bioorg. Med. Chem*. **2008**, *16*, 2968–2973.

(17) Camps, P.; Formosa, X.; Galdeano, C.; Gomez, T.; Munoz-Torrero, D.; Scarpellini, M.; Viayna, E.; Badia, A.; Victoria Clos, M.; Camins, A.; Pallas, M.; Bartolini, M.; Mancini, F.; Andrisano, V.; Estelrich, J.; Lizondo, M.; Bidon-Chanal, A.; Luque, F. J. Novel donezepil-based inhibitors of acetyl- and butyrylcholinesterase and acetylcholinesterase-induced β-amyloid aggregation. *J. Med. Chem*. **2008**, *51*, 3588–3598.

(18) Fang, L.; Appenroth, D.; Decker, M.; Kiehntopf, M.; Roegler, C.; Deufel, T.; Fleck, C.; Peng, S.; Zhang, Y.; Lehmann, J. Synthesis and biological evaluation of NO-donor-tacrine hybrids as hepatoprotective anti-Alzheimer drug candidates. *J. Med. Chem*. **2008**, *51*, 713–716.

(19) (a) Marco-Contelles, J.; Leon, R.; de los Rios, C.; Guglietta, A.; Terencio, J.; Lopez, M. G.; Garcia, A. G.; Villarroya, M. Novel multipotent tacrine−dihydropyridine hybrids with improved acetylcholinesterase inhibitory and neuroprotective activities as potential drugs for the treatment of Alzheimer's disease. *J. Med. Chem*. **2006**, *49*, 7607–7610. (b) Leon, R.; de los Rios, C.; Marco-Contelles, J.; Huertas, O.; Barril, X.; Luque, F. J.; Lopez, M. G.; Garcia, A. G.; Villarroya, M. New tacrine−dihydropyridine hybrids that inhibit acetylcholinesterase, calcium entry and exhibit neuroprotection properties. *Bioorg. Med. Chem*. **2008**, *16*, 7759–7769.

(20) Rodriguez-Franco, M. I.; Fernandez-Bachiller, M. I.; Pérez, C.; Hernandez-Ledesma, B.; Bartolomé, B. Novel tacrine−melatonin hybrids as dual-acting drugs for Alzheimer disease, with improved acetylcholinesterase inhibitory and antioxidant properties. *J. Med. Chem*. **2006**, *49*, 459–462.

(21) Sterling, J.; Herzig, Y.; Goren, T.; Finkelstein, N.; Lerner, D.; Goldenberg, W.; Miskolczi, I.; Molnar, S.; Rantal, F.; Tamas, T.; Toth, G.; Zagyva, A.; Zekany, A.; Lavian, G.; Gross, A.; Friedman, R.; Razin, M.; Huang, W.; Krais, B.; Chorev, M.; Youdim, M. B.; Weinstock, M. Novel dual inhibitors of AChE and MAO derived from hydroxy aminoindan and phenylethylamine as potential treatment for Alzheimer's disease. *J. Med. Chem*. **2002**, *45*, 5260–5279.

(22) Toda, N.; Tago, K.; Marumoto, S.; Takami, K.; Ori, M.; Yamada, N.; Koyama, K.; Naruto, S.; Abe, K.; Yamazaki, R.; Hara, T.; Aoyagi, A.; Abe, Y.; Kaneko, T.; Kogen, H. A conformational restriction approach to the development of dual inhibitors of acetylcholinesterase and serotonin transporter as potential agents for Alzheimer's disease. *Bioorg. Med. Chem*. **2003**, *11*, 4389–4415.

(23) Fang, L.; Kraus, B.; Lehmann, J.; Heilmann, J.; Zhang, Y.; Decker, M. Design and synthesis of tacrine−ferulic acid hybrids as multi-potent anti-Alzheimer drug candidates. *Bioorg. Med. Chem. Lett*. **2008**, *18*, 2905–2909.

(24) Rizzo, S.; Rivière, C.; Piazzi, L.; Bisi, A.; Gobbi, S.; Bartolini, M.; Andrisano, V.; Morroni, F.; Tarozzi, A.; Monti, J. P.; Rampa, A. Benzofuran-based hybrid compounds for the inhibition of cholinesterase activity, β-amyloid aggregation, and Aβ neurotoxicity. *J. Med. Chem.* **2008**, *51*, 2883–2886.

(25) Lange, J. H. M.; Coolen, H. K. A. C.; van Stuivenberg, H. H.; Dijksman, J. A. R.; Herremans, A. H. J.; Ronken, E.; Keizer, H. G.; Tipker, K.; McCreary, A. C.; Veerman, W.; Wals, H. C.; Stork, S.; Verveer, P. C.; den Hartog, A. P.; de Jong, N. M. J.; Adolfs, T. J. P.; Hoogendoorn, J.; Kruse, C. G. Synthesis, biological properties and molecular modeling investigations of novel 3,4-diarylpyrazolines as potent and selective CB_1 cannabinoid receptor antagonists. *J. Med. Chem.* **2004**, *47*, 627–643.

(26) (a) Lange, J. H. M.; van Stuivenberg, H. H.; Veerman, W.; Wals, H. C.; Stork, B.; Coolen, H. K. A. C.; McCreary, A. C.; Adolfs, T. J. P.; Kruse, C. G. Novel 3,4-diarylpyrazolines as potent cannabinoid CB_1 receptor antagonists with lower lipophilicity. *Bioorg. Med. Chem. Lett.* **2005**, *15*, 4794–4798. (b) Lange, J. H. M.; Kruse, C. G. Cannabinoid CB_1 receptor antagonists in therapeutic and structural perspectives. *Chem. Rec.* **2008**, *8*, 156–168.

(27) Smith, R. A.; O'Connor, S. J.; Wirtz, S. N.; Wong, W. C.; Choi, S.; Klünder, H. C.; Ning, S.; Wang, G.; Achebe, F; Ying, S. Imidazole-4-carboxamide Derivatives, Preparation and Use Thereof for the Treatment of Obesity. WO03/040107, **2003**.

(28) Lange, J. H. M.; van Stuivenberg, H. H.; Coolen, H. K. A. C.; Adolfs, T. J. P.; McCreary, A. C.; Keizer, H. G.; Wals, H. C.; Veerman, W.; Borst, A. J. M.; De Looff, W.; Verveer, P. C.; Kruse, C. G. Bioisosteric replacements of the pyrazole moiety of rimonabant: synthesis, biological properties and molecular modeling investigations of thiazoles, triazoles and imidazoles as potent and selective CB_1 cannabinoid receptor antagonists. *J. Med. Chem.* **2005**, *48*, 1823–1838.

(29) (a) Reggio, P. H. Pharmacophores for ligand recognition and activation/inactivation of the cannabinoid receptors. *Curr. Pharm. Des.* **2003**, *9*, 1607–1633. (b) Lange, J. H. M.; Kruse, C. G. Recent advances in CB_1 cannabinoid receptor antagonists. *Curr. Opin. Drug Discovery Dev.* **2004**, *7*, 498–506. (c) Lange, J. H. M.; Kruse, C. G. Medicinal chemistry strategies to CB_1 cannabinoid receptor antagonists. *Drug Discovery Today* **2005**, *10*, 693–702. (d) Wang, H.; Duffy, R. A.; Boykow, G. C.; Chackalamannil, S.; Madison, V. S. Identification of novel cannabinoid CB1 receptor antagonists by using virtual screening with a pharmacophore model. *J. Med. Chem.* **2008**, *51*, 2439–2446. (e) Foloppe, N.; Benwell, K.; Brooks, T. D.; Kennett, G.; Knight, A. R.; Misra, A.; Monck, N. J. T. Discovery and functional evaluation of diverse novel human CB_1 receptor ligands. *Bioorg. Med. Chem. Lett.* **2009**, *19*, 4183–4190.

(30) Jagerovic, N.; Fernandez Fernandez, C.; Goya Laza, M. P.; Callado Hernando, L. F.; Meana Marinez, J. J. Pyrazolecarboxamide Derivatives, Method of Obtaining Same and Use Thereof as Inverse Antagonists/Agonists of the Cannabinoid CB_1 and Opioid Mu Receptor. WO2007/028849, **2007**.

(31) (a) Cichewicz, D. L.; Martin, Z. L.; Smith, F. L.; Welch, S. P. Enhancement of μ opioid antinociception by oral Δ^9-tetrahydrocannabinol: dose-response analysis and receptor identification. *J. Pharmacol. Exp. Ther.* **1999**, *289*, 859–867. (b) Tham, S. M.; Angus, J. A.; Tudor, E. M.; Wright, C. E. Synergistic and additive interactions of the cannabinoid agonist CP55,940 with μ-opioid receptor and α_2-adrenoceptor agonists in acute pain models in mice. *Br. J. Pharmacol.* **2005**, *144*, 875–884.

(32) Rydberg, E. H.; Brumstein, B.; Greenblatt, H. M.; Wong, D. M.; Shaya, D.; Williams, L. D.; Carlier, P. R.; Pang, Y.-P.; Silman, I.; Sussman, J. L. Complexes of alkylene-linked tacrine dimers with torpedo Californica acetylcholinesterase: binding of bis(5)-tacrine produces a dramatic rearrangement in the active-site gorge. *J. Med. Chem.* **2006**, *49*, 5491–5500.

(33) Harel, M.; Schalk, I.; Ehret-Sabatier, L.; Bouet, F.; Goeldner, M.; Hirth, C.; Axelsen, P. H.; Silman, I.; Sussman, J. L. Quaternary ligand binding to aromatic residues in the active-site gorge of acetylcholinesterase. *Proc. Natl. Acad. Sci. U.S.A.* **1993**, *90*, 9031–9035.

(34) Carlier, P. R.; Chow, E. S.-H.; Han, Y.; Liu, J.; El Yazal, J.; Pang, J.-P. Heterodimeric tacrine-based acetylcholinesterase inhibitors: investigating ligand−peripheral site interactions. *J. Med. Chem.* **1999**, *42*, 4225–4231.

(35) Lan, R.; Liu, Q.; Fan, P.; Lin, S.; Fernando, S. R.; McCallion, D.; Pertwee, R.; Makriyannis, A. Structure−activity relationships of pyrazole derivatives as cannabinoid receptor antagonists. *J. Med. Chem.* **1999**, *42*, 769–776.

(36) (a) Shim, J.-Y.; Welsh, W. J.; Howlett, A. C. Homology model of the CB1 cannabinoid receptor: sites critical for nonclassical cannabinoid agonist interaction. *Biopolymers* **2003**, *71*, 169–189. (b) Hurst, D. P.; Lynch, D. L.; Barnett-Norris, J.; Hyatt, S. M.; Seltzman, H. H.; Zhong, M.; Song, Z.-H.; Nie, J.; Lewis, D.; Reggio, P. H. *N*-(Piperidin-1-yl)-5-(4-chlorophenyl)-1-(2,4-dichlorophenyl)-4-methyl-1*H*-pyrazole-3-carboxamide (SR141716A) interaction with LYS 3.28(192) is crucial for its inverse agonism at the cannabinoid receptor. *Mol. Pharmacol.* **2002**, *62*, 1274–1287. (c) McAllister, S. D.; Rizvi, G.; Anavi-Goffer, S.; Hurst, D. P.; Barnett-Norris, J.; Lynch, D. L.; Reggio, P. H.; Abood, M. E. An aromatic microdomain at cannabinoid CB_1 receptor constitutes an agonist/inverse agonist binding region. *J. Med. Chem.* **2003**, *46*, 5139–5152. (d) Salo, O. M. H.; Lahtela-Kakkonen, M.; Gynther, J.; Järvinen, T.; Poso, A. Development of a 3D model for the human cannabinoid CB1 receptor. *J. Med. Chem.* **2004**, *47*, 3048–3057. (e) Srivastava, B. K.; Joharapurkar, A.; Raval, S.; Patel, J. Z.; Soni, R.; Raval, P.; Gite, A.; Goswami, A.; Sadhwani, N.; Gandhi, N.; Mishra, B.; Solanki, M.; Pandey, B.; Jain, M. R.; Patel, P. R. Diaryl dihydropyrazole-3-carboxamides with significant in vivo antiobesity activity related to CB1 receptor antagonism: synthesis, biological evaluation, and molecular modeling in the homology model. *J. Med. Chem.* **2007**, *50*, 5951–5966. (f) Lin, L. S.; Ha, S.; Ball, R. G.; Tsou, N. N.; Castonguay, L. A.; Doss, G. A.; Fong, T. M.; Shen, C.-P.; Xiao, J. C.; Goulet, M. T.; Hagmann, W. K. Conformational analysis and receptor docking of N-[(1S,2S)-3-(4-chlorophenyl)-2-(3-cyanophenyl)-1-methylpropyl]-2-methyl-2-{[5-(trifluoromethyl)pyridine-2-yl]oxy}propanamide (taranabant, MK-0364), a novel, acyclic cannabinoid-1 receptor inverse agonist. *J. Med. Chem.* **2008**, *51*, 2108–2114.

(37) Cherezov, V.; Rosenbaum, D. M.; Hanson, M. A.; Rasmussen, S. G.; Thian, F. S.; Kobilka, T. S.; Choi, H. J.; Kuhn, P.; Weis, W. I.; Kobilka, B. K.; Stevens, R. C. High-resolution crystal structure of an engineered human beta2-adrenergic G protein-coupled receptor. *Science* **2007**, *318*, 1258–1265.

(38) *ACD/pK_a DB*, version 11.01; Advanced Chemistry Development, Inc.: Toronto, Ontario, Canada, 2007; www.acdlabs.com.

(39) Patocka, J.; Jun, D.; Kuca, K. Possible roles of hydroxylated metabolites of tacrine in drug toxicity and therapy of Alzheimer's disease. *Curr. Drug Metab.* **2008**, *9*, 332–335.

(40) Li, W. M.; Kan, K. K. W.; Carlier, P. R.; Pang, Y. P.; Han, Y. F. East meets West in the search for Alzheimer's therapeutics: novel dimeric inhibitors from tacrine and huperzine A. *Curr. Alzheimer's Res.* **2007**, *4*, 386–396.

(41) Meschler, J. P.; Kraichely, D. M.; Wilken, G. H.; Howlett, A. C. Inverse agonist properties of *N*-(piperidin-1-yl)-5-(4-chlorophenyl)-1-(2,4-dichlorophenyl)-4-methyl-1*H*-pyrazole-3-carboxamide HCl (SR141716A) and 1-(2-chlorophenyl)-4-cyano-5-(4-methoxyphenyl)-1*H*-pyrazole-3-carboxylic acid phenylamide (CP272871) for the CB_1 cannabinoid receptor. *Biochem. Pharmacol.* **2000**, *60*, 1315–1323.

(42) Kenakin, T. Inverse, protean, and ligand-selective agonism: matters of receptor conformation. *FASEB J.* **2001**, *15*, 598–611.

(43) Bond, R. A.; IJzerman, A. P. Recent developments in constitutive receptor activity and inverse agonism, and their potential for GPCR drug discovery. *Trends Pharmacol. Sci.* **2006**, *27*, 92–96.

(44) Ellman, G. L.; Courtney, K. D.; Andrés, B. J.; Featherstone, R. M. A new and rapid colorimetric determination of acetylcholinesterase activity. *Biochem. Pharmacol.* **1961**, *7*, 88–95.